# 4*f* spin density in the reentrant ferromagnet $SmMn_2Ge_2$

J. E. McCarthy,[1] J. A. Duffy,[2,*] C. Detlefs,[1] M. J. Cooper,[2] and P. C. Canfield[3]
[1]*European Synchrotron Radiation Facility, BP 220, F-38043 Grenoble, France*
[2]*Department of Physics, University of Warwick, Coventry CV4 7AL, United Kingdom*
[3]*Ames Laboratory, 59 Physics, Iowa State University, Ames, Iowa 50011*
(Received 7 June 2000)

The spin contribution to the magnetic moment in $SmMn_2Ge_2$ has been measured by magnetic Compton scattering in both the low- and high-temperature ferromagnetic phases. At low temperature, the Sm site is shown to possess a large $4f$ spin moment of $3.4\pm0.1\mu_B$, aligned antiparallel to the total magnetic moment. At high temperature, the data show conclusively that ordered magnetic moments are present on the samarium site.

The ternary compounds of structure $RT_2X_2$, where $R$ is a rare earth, $T$ is a transition metal, and $X$ is either Si or Ge, are of considerable interest since they exhibit a wide variety of phenomena, ranging from heavy fermion behavior and superconductivity to strong ferro- and antiferromagnetism.[1,2] The $RMn_2Ge_2$ subseries is of particular interest as the transition metal carries a magnetic moment. These compounds crystallize in the $ThCr_2Si_2$-type body-centered tetragonal structure consisting of layers stacked along the $c$ axis in the sequence $R$-Ge-$Mn_2$-Ge-$R$ (Refs. 1 and 2). The magnetic ordering depends critically on the planar Mn-Mn distance, $d$. For values greater than $d_c=2.87$ Å ferromagnetism is observed, whereas below this antiferromagnetic ordering is favored. In $SmMn_2Ge_2$, $d$ is approximately equal to this critical value,[3] and numerous magnetization measurements[4,5] have shown a complex temperature dependence of the magnetic ordering in the compound. Furthermore, this material exhibits giant magnetoresistance of magnitude $\approx 8\%$ associated with the antiferromagnetic phase.[6] As a naturally layered material, the properties of $SmMn_2Ge_2$ provide an interesting complement to studies of artificial multilayer materials.

The purpose of the present study was to determine the moments on the Sm site at different temperatures. The spin moments on the Sm and Mn sites were determined by fitting atomic models to the magnetic Compton profiles (MCP's).

One of the key objectives of earlier work has been to determine the different magnetic structures of this material at various temperatures.[3–5,7–9] $SmMn_2Ge_2$ has three magnetically ordered phases. At 345 K (above which it is paramagnetic), the material becomes ferromagnetic. Below 155 K, antiferromagnetic ordering occurs, and remains for temperatures down to 105 K (Ref. 9), then the compound becomes ferromagnetic once more. The ordering is strongly anisotropic: in the high-temperature ferromagnetic phase, the easy axis lies along the [001] direction but along the [110] direction in the low-temperature ferromagnetic phase. A further phase transition has been suggested at $T_c\approx 30$ K and was thought to arise from an ordering of the Sm magnetic moment.[3]

Very recently, Tomka *et al.*[9] used powder neutron diffraction to study the origin of the magnetic moments in this material. They revealed a complex noncollinear buckled structure with net ferromagnetic components of $\approx 2\mu_B$ per Mn and up to $0.65\mu_B$ per Sm site. It was shown that the Mn moments are not aligned with any high-symmetry direction of the crystal, and that the change in orientation of the easy magnetization axis results from a change of the coupling, which leads to cancellation of the net ferromagnetic moment components within the basal plane or along [001] in the high- and low-temperature phases, respectively. These measurements were performed on isotopically enriched samples in order to minimize the prohibitive neutron absorption in natural samarium. Tomka *et al.* derived these results from a Rietveld refinement which relies on tabulated values for the neutron magnetic form factors. They assumed the Sm moment to be induced by the Mn net ferromagnetic moment and therefore they refined only its collinear projection. While Tomka *et al.* were mostly concerned with the Mn antiferromagnetism, our current work focuses on the distribution of the net ferromagnetic moments, mainly on the Sm sublattice. For more details on the antiferromagnetic structures, we refer the reader to Ref. 9.

Samarium has electronic configuration $4f^5$, and its Hund's rules ground state is predicted to have a small total moment of $0.84\mu_B$ arising from large antiparallel spin ($S=5/2$) and orbital ($L=5$) angular momenta. However, another $J$ multiplet lies just above this free-ion ground state, and crystalline electric field (CEF) effects frequently lead to different ground states: hence Hund's rules are expected to be unreliable in this system. Indeed in pure Sm metal the paramagnetic moment is observed to be $1.5\mu_B$, instead of the $0.84\mu_B$ expected. Consequently, knowledge of the spin and orbital moments is particularly important in order to understand the magnetization of this material. Magnetic form factors are sensitive to the assumed $S$ and $L$ values of the magnetic ground state, leading to uncertainties in the total Sm moment derived from neutron powder data. X-ray magnetic circular dichroism (XMCD) is not an ideal technique in this case because the validity of the sum rules is not well established for the investigation of $4f$ materials. This magnetic Compton scattering (MCS) measurement, however, provides this essential information directly and unambiguously.

 

MCS is a uniquely sensitive probe of the spin component of the magnetization. The Compton effect is observed when high-energy photons are scattered off electrons. For bound electrons which have some distribution of momenta, the scattered photon energy is Doppler broadened into an energy distribution. The Compton profile, $J(p_z)$, is defined as the one-dimensional projection of the electron momentum distribution, $n(\mathbf{p})$, onto the scattering vector, taken to be parallel to the $z$ direction:

$$J(p_z)=\int\int n(\mathbf{p})dp_x dp_y . \tag{1}$$

Within the impulse approximation,[10] the Compton profile is directly proportional to the scattering cross section.[11] The integral of $J(p_z)$ is simply the total number of electrons per unit cell. If the photons impinging on a sample have a component of circular polarization, then a small spin dependence appears in the scattering cross section.[12] Reversing either the photon polarization or the magnetization of the sample changes the sign of the spin-dependent signal, which enables the spin part to be isolated. The resultant magnetic Compton profile (MCP), is a projection of the momentum density of only those electrons with unpaired spins,

$$J_{\mathrm{mag}}(p_z)=\int\int [n^{\uparrow}(\mathbf{p})-n^{\downarrow}(\mathbf{p})]dp_x dp_y . \tag{2}$$

Here, $n^{\uparrow}(\mathbf{p})$ and $n^{\downarrow}(\mathbf{p})$ are the momentum-dependent majority and minority spin densities, respectively. The area under the MCP is equal to the number of unpaired electrons, i.e., the total spin moment per formula unit in Bohr magnetons.

Magnetic Compton scattering is now an established technique for probing momentum space-spin densities and band structures in magnetic materials.[13,14] Within the impulse approximation, the method is solely sensitive to *spin* magnetic moments, $S$ (Refs. 13, 15 and 16); the orbital moment, $L$, is not measured.[17] This is especially useful in the light rare earths and actinides, where $J=L-S$ may be small, even if $L$ and $S$ are large. Unlike XMCD, MCS is equally sensitive to all spin-polarized electrons, regardless of their binding energy and the symmetry of their wave functions. Since the MCP is a difference between Compton profiles, the contributions from the spin-paired electrons and from unwanted systematic sources cancel out. In the study of Sm and related materials, high-energy x rays have the additional advantage that they do not suffer from the large absorption factors associated with neutrons, which have severely hindered such experiments.[9]

The basal plane MCP for $SmMn_2Ge_2$ was measured on the high-energy x-ray beamline, ID15, of the ESRF. The experiment was performed in reflection geometry[18] with a scattering angle of 168°. The incident beam energy of 296 keV was selected by the {311} reflection of a Si monochromator. The sample was grown by the slow cooling of a ternary melt rich in Mn and Ge (Ref. 19). For the experiment a piece of dimensions $5\times3\times1.5$ mm$^3$ was cut from the resultant crystal and was oriented so that the resolved direction was in the basal plane to within $\pm2°$.

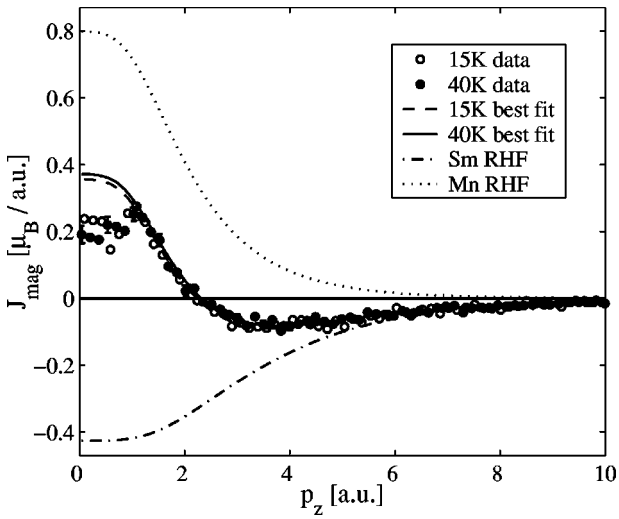


FIG. 1. The experimental magnetic Compton profile of $SmMn_2Ge_2$ at $T=15$ K and $T=40$ K. The fits were performed for $p_z>1.5$ a.u., using RHF predictions for the Mn $3d$ and Sm $4f$ moment, convoluted with a Gaussian of full width at half maximum $=0.44$ a.u. to represent the experimental resolution.

The temperature of the sample was maintained at $15\pm2$ K, $40\pm2$ K, and $230\pm2$ K for the three measurements. The sample's magnetization was reversed with a 0.96 T rotating permanent magnet. For the two low-temperature measurements, this was sufficient to saturate the magnetic moment, while at 230 K the moment was approximately 50% saturated, since in the high-temperature ferromagnetic phase the easy axis is perpendicular to the basal plane. A degree of circular polarization of $P_c\approx45\%$ was obtained by selecting a beam 20 $\mu$rad above the orbital plane of the synchrotron. The energy spectrum of the scattered x rays was measured by a solid-state Ge detector. The momentum resolution obtained was 0.44 atomic units (a.u., where 1 a.u.$=1.99\times10^{-24}$ kg m s$^{-1}$). The total number of counts in each of the charge profiles was $1.5\times10^8$, resulting in $3.7\times10^6$ in the MCP with a statistical precision of $\pm3\%$ at the magnetic Compton peak in a bin of width 0.09 a.u. The usual correction procedures[20] for the energy dependence of the detector efficiency, absorption, the relativistic scattering cross section, and magnetic multiple scattering were applied, and after checking that the profiles were symmetric about zero momentum, the MCP's were folded about this point to increase the effective statistical precision of the data. The amplitude of the MCP spectra, $J_{\mathrm{mag}}(p_z)$, was calibrated using data for Fe and Ni obtained under the same experimental conditions to correct for the partial circular polarization of the incident beam and other geometrical factors.

The results from the measurements at 15 and 40 K are shown in Fig. 1, together with model profiles for Sm $4f$ and Mn $3d$ electrons based on relativistic Hartree Fock (RHF) free atom wave functions.[21] The model profiles have been scaled to provide a best least-squares fit to the data for $p_z>1.5$ a.u. The fact that these free atom model profiles must provide an accurate description of the Compton profiles at high momentum results from energy considerations. The kinetic energy of the electron distribution is given by the second moment of the Compton profile. The virial theorem ensures that the kinetic energy and the total energy are

TABLE I. The magnetic moments associated with Sm and Mn at 15 K and 40 K.

| Moments [$\mu_B$/formula unit] | 15 K | 40 K |
|---|---|---|
| Total spin | $-0.01(3)$ | $+0.02(3)$ |
| Sm spin | $-3.5(1)$ | $-3.4(1)$ |
| Mn+delocalized spin | $+3.5(1)$ | $+3.4(1)$ |
| Total magnetization | $+4.1$ | $+4.1$ |
| Total orbital | $+4.1$ | $+4.1$ |

numerically equal but opposite in sign. Therefore the very small total energy changes responsible for cohesion derive from changes in the electron distribution at low momenta, associated with electron density away from the atomic cores. The profiles for Mn $3d$ and Sm $4f$ electrons are significantly different, the latter being 50% broader, and therefore fitting at high momenta can be used to separate the moments. This difference can be thought of as simply arising from the fact that the Sm $4f$ electrons are more tightly bound than the Mn $3d$ electrons, and this difference manifests itself in higher momentum components for the $4f$ against the $3d$ electrons: a result which is also evident from simple consideration of the uncertainty principle.

The analysis of magnetic Compton line shapes in terms of the characteristically different orbital profiles has been demonstrated in many similar cases, e.g., $HoFe_2$,[20] $CeFe_2$,[22] and $UFe_2$.[23] Our results presented in Fig. 1 clearly show that there is a large negative $4f$ spin moment, opposed to the positive Mn $3d$ moment. Even though the magnetic configuration of Sm is sensitive to the CEF environment, the MCP's of Sm and other $4f$ materials indicate that deviations from the atomic behavior are small, a result also supported by neutron-diffraction data. Thus the area under the fitted $4f$ curve gives a reliable estimate of the Sm spin moment. Combination of bulk magnetization data with the measured spin moments allow us to infer the size of the orbital moment. These values, given in Table I were determined as follows.

The total spin moment, calculated simply by integrating the MCP, is effectively zero for the 15 and 40 K data. The area under the Sm $4f$ profile at 40 K was deduced to be $3.4\pm0.1\mu_B$ per formula unit. This means that the spin moment associated with the Mn $3d$ electrons together with the delocalized electrons, also amounts to the same value, $3.4\mu_B$ per formula unit, but aligned antiparallel. Note that the fitted Mn $3d$ profile (dotted line in (Fig. 1) is inappropriate at low momenta ($p_z<1.5$ a.u.) because the $3d$ electrons are sensitive to the solid-state environment, and their contribution will differ from free-atom behavior, unlike the Sm $4f$ electrons. In addition small contributions at low momentum from both delocalized Mn ($4sp$-like) and Sm ($5d$- and $6sp$-like) electrons, are evident in Fig. 1 from the discrepancy between the data and the fitted curve at low momentum. Similar effects are found in studies on other $3d$ systems,[24] and an electronic structure calculation would be needed to examine this further. The main interpretation of this MCP is that there is a Sm $4f$ spin moment of $3.4\mu_B$, which is aligned antiparallel to the Mn $3d$ and total magnetizations. Since the total spin moment is zero, we can also deduce the size of the orbital moment in this material. In order to account for the macroscopic ferromagnetic moment of $4.1\mu_B$ measured by

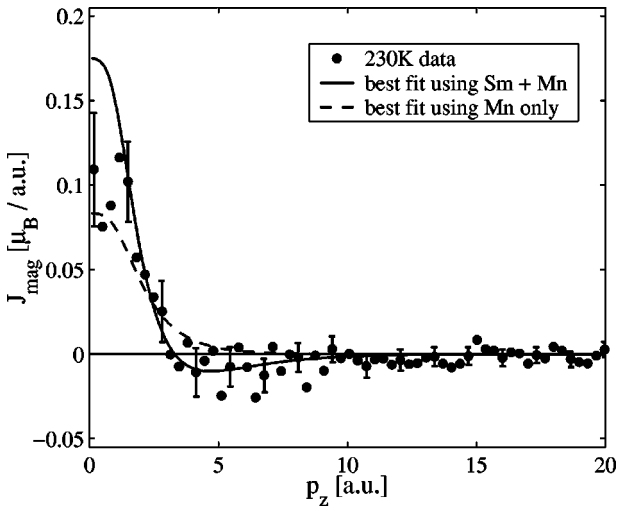


FIG. 2. The experimental magnetic Compton profile of $SmMn_2Ge_2$ at $T=230$ K. The lines represent the fitted RHF profiles obtained using the least-squares method for Mn $3d$ electrons only and both Sm $4f$ and Mn $3d$ electrons. These fits clearly indicate the presence of a Sm $4f$ contribution.

superconducting quantum interference device magnetometry there must be an orbital moment of this size. This orbital moment is aligned with the total magnetization, i.e., parallel to the Mn spin direction. A large orbital contribution is expected from the Sm $4f$ shell ($L=5$), while the orbital moment of delocalized electrons is usually quenched. The transition metals represent an intermediate case, where spin-orbit coupling and CEF effects are of comparable strength, therefore a $3d$ orbital moment will be reduced, but cannot be ruled out completely, as has been shown recently in NiO (Ref. 25). In the $Mn^{2+}$ ion the $3d$ shell is exactly half filled ($S=5/2$, $L=0$), so that the orbital moment vanishes. In $SmMn_2Ge_2$, however, the valence of Mn is not known, so that an orbital moment on the Mn site cannot be neglected *a priori*. Nevertheless, the comparison of MCP's and bulk magnetization clearly shows that at low temperature there is a significant contribution from orbital moments, even though from the present measurements we cannot determine its origin,

The moments determined for the 15 K data (Fig. 1) and given in Table I show that no significant difference was observed between the 15 and 40 K profiles. Hence, we observe no evidence of the reordering of the Sm moment between these temperatures proposed by Sampathkumaran *et al.*[3]

In Fig. 2 we present preliminary MCP data measured at $T=230$ K. Despite the poorer statistical accuracy it is clear that the data are still negative for momenta above 3 a.u.; in fact the area in the region $4<p_z<10$ a.u. is $-0.04\pm0.01\mu_B$. The Sm $4f$ spin moment is reduced compared with the low-temperature data. The lines shown in Fig. 2 represent fits to the data points first assuming there is no Sm spin moment present (dashed line) and then assuming contributions from both Sm $4f$ and Mn $3d$ electrons (solid line). The least-squares fit was made in the momentum range $1.5<p_z<15$ a.u., i.e., beyond the low momentum region where solid-state effects reduce the Mn moment. The curve obtained using Mn only clearly does not represent a good fit to the data, whereas the data points show a normal distribution

about the fit including both Sm and Mn contributions, which yields a Sm spin moment of $0.7 \pm 0.1 \mu_B$, again aligned antiparallel to the total and Mn $3d$ magnetizations. The Sm spin moment has been observed conclusively in the high-temperature phase in this material. A vanishing Sm moment at high temperature could not be excluded in the neutron data of Tomka *et al.*[9] since the refinement procedure was consistent with moment values ranging from zero to $0.6\mu_B$. It should also be noted that since the *total* moment, measured by neutrons, is much smaller than the spin and orbital contributions, the magnetic Compton scattering experiment is more sensitive to the existence of any ferromagnetic ordering. Furthermore, the MCP result does not rely on complex data analysis; it can be deduced directly from the raw data. The negative tail of the MCP's shown in Figs. 1 and 2 cannot be interpreted without a negative $4f$ contribution to the moment.

The bulk magnetization at 230 K and 0.96 T was measured to be $2.1\mu_B$. Together with the spin component measured by MCP, $0.7\mu_B$, this means that there has to be an orbital magnetic moment of $1.4\mu_B$. Where this unexpectedly large orbital moment originates is the subject of ongoing research.

In conclusion, our results show that in the low-temperature ferromagnetic phase there is a large spin moment of $3.4 \pm 0.1 \mu_B$, negatively polarized with respect to the Mn spin moment and total magnetization. This, together with the magnetization data, means that there is also a large orbital moment of similar size. Our data do not support the existence of a magnetic phase transition near $T = 30$ K. At high temperature, a Sm $4f$ moment definitely exists, albeit reduced in size from the low-temperature value.

We would like to thank the ESRF for provision of beam time, and the EPSRC (UK) for financial support. We also thank Clemens Ritter for critical reading of the manuscript and helpful discussions, and Martin Lees for performing magnetization measurements at Warwick. The Ames Laboratory is operated for the US DOE under Contract No. W-7405-ENG-82. This work was supported by the Director-ate for Energy Research, Office of Basic Energy Sciences.

*Present Address: H.H. Wills Physics Laboratory, University of Bristol, Tyndall Avenue, Bristol BS8 1TL, UK.

[1] A. Szytula and J. Leciejewicz, *Handbook of Crystal Structures and Magnetic Properties of Rare Earth Intermetallics* (CRC Press, Boca Raton, 1994), pp. 114–192.

[2] A. Szytula and J. Leciejewicz, in *Handbook on the Physics and Chemistry of Rare Earths*, edited by K.A. Gschneidner, Jr. and L. Eyring (Elsevier Science, Amsterdam, 1989), Vol. 12, pp. 133–211.

[3] E.V. Sampathkumaran, P.L. Paulose, and R. Mallik, Phys. Rev. B **54**, R3710 (1996).

[4] H. Fujii, T. Okamoto, T. Shigeoka, and N. Iwata, Solid State Commun. **53**, 715 (1985).

[5] E.M. Gyorgy, B. Batlogg, J.P. Remeika, R.B. van Dover, R.M. Fleming, H.E. Bair, G.P. Espinosa, A.S. Cooper, and R.G. Maines, J. Appl. Phys. **61**, 4237 (1987).

[6] R.B. van Dover, E.M. Gyorgy, R.J. Cava, J.J. Krajewski, R.J. Felder, and W.F. Peck, Phys. Rev. B **47**, 6134 (1993).

[7] J.S. Lord, P.C. Riedi, G.J. Tomka, Cz. Kapusta, and K.H.J. Buschow, Phys. Rev. B **53**, 283 (1996).

[8] G.J. Tomka, Cz. Kapusta, C. Ritter, P.C. Riedi, R. Cywinski, and K.H.J. Buschow, Physica B **230-232**, 727 (1997).

[9] G.J. Tomka, C. Ritter, P.C. Riedi, Cz. Kapusta, and W. Kocemba, Phys. Rev. B **58**, 6330 (1998).

[10] P.M. Platzman and N. Tzoar, Phys. Rev. B **2**, 3556 (1970).

[11] P. Holm, Phys. Rev. A **37**, 3706 (1988).

[12] F. Bell, J. Felsteiner, and L.P. Pitaevskii, Phys. Rev. A **53**, R1213 (1996).

[13] N. Sakai, J. Appl. Crystallogr. **29**, 81 (1996).

[14] M.J. Cooper, Radiat. Phys. Chem. **50**, 63 (1997).

[15] M.J. Cooper, E. Zukowski, S.P. Collins, D.N. Timms, F. Itoh, and H. Sakurai, J. Phys.: Condens. Matter **4**, L399 (1992).

[16] S.W. Lovesey, J. Phys.: Condens. Matter **8**, L353 (1996).

[17] P. Carra, M. Fabrizio, G. Santoro, and B.T. Thole, Phys. Rev. B **53**, R5994 (1996).

[18] J.A. Duffy, J.E. McCarthy, S.B. Dugdale, V. Honkimäki, M.J. Cooper, M.A. Alam, T. Jarlborg, and S.B. Palmer, J. Phys.: Condens. Matter **10**, 10 391 (1998).

[19] P.C. Canfield and Z. Fisk, Philos. Mag. B **65**, 3151 (1992).

[20] E. Zukowski, S.P. Collins, M.J. Cooper, D.N. Timms, F. Itoh, H. Sakurai, H. Kawata, Y. Tanaka, and A. Maliowski, J. Phys.: Condens. Matter **5**, 4077 (1993).

[21] F. Biggs, L.B. Mendelsohn, and J.B. Mann, At. Data Nucl. Data Tables **16**, 201 (1975).

[22] M.J. Cooper, P.K. Lawson, M.A.G. Dixon, E. Zukowski, D.N. Timms, F. Itoh, H. Sakurai, H. Kawata, Y. Tanaka, and M. Ito, Phys. Rev. B **54**, 4068 (1996).

[23] P.K. Lawson, M.J. Cooper, M.A.G. Dixon, D.N. Timms, E. Zukowski, F. Itoh, and H. Sakurai, Phys. Rev. B **56**, 3239 (1997).

[24] M.A.G. Dixon, J.A. Duffy, S. Gardelis, J.E. McCarthy, M.J. Cooper, S.B. Dugdale, T. Jarlborg, and D.N. Timms, J. Phys.: Condens. Matter **10**, 2759 (1998).

[25] V. Fernandez, C. Vettier, F. de Bergevin, C. Giles, and W. Neubeck, Phys. Rev. B **57**, 7870 (1998); W. Neubeck, C. Vettier, V. Fernandez, F. de Bergevin, and C. Giles, J. Appl. Phys. **85**, 4847 (1999).